Environ Sci Pollut Res (2012) 19:4016–4029
DOI 10.1007/s11356-012-0970-5

RESEARCH ARTICLE

Variations of surface O_3 in August at a rural site near Shanghai: influences from the West Pacific subtropical high and anthropogenic emissions

Jingwei He · Yuxuan Wang · Jiming Hao · Lulu Shen · Long Wang

Received: 7 January 2012 / Accepted: 7 May 2012 / Published online: 31 May 2012

Abstract Large day-to-day variability in O_3 and CO was observed at Chongming, a remote rural site east of Shanghai, in August 2010. High ozone periods (HOPs) that typically lasted for 3–5 days with daily maximum ozone exceeding 102 ppb were intermittent with low ozone periods (LOPs) with daily maximum ozone less than 20 ppb. The correlation analysis of ozone with meteorological factors suggests that the large variations of surface ozone are driven by meteorological conditions correlated with the changes in the location and intensity of the west Pacific subtropical high (WPSH) associated with the East Asian summer monsoon (EASM). When the center of WPSH with weaker intensity is to the southeast of Chongming site, the mixing ratios and variability of surface ozone are higher. When the center of WPSH with stronger intensity is to the northeast of Chongming site, the mixing ratios and variability of surface ozone are lower. Sensitivity simulations using the GEOS-Chem chemical transport model indicate that meteorological condition associated with WPSH is the primary factor controlling surface ozone at Chongming in August, while local anthropogenic emissions make significant contributions to surface ozone concentrations only during HOP.

Keywords Ozone pollution · Temperature inversion · West Pacific subtropical high (WPSH) · East China · Anthropogenic emissions

Responsible editor: Euripides Stephanou

J. He · Y. Wang · J. Hao · L. Shen
Ministry of Education Key Laboratory for Earth System Modeling, Center for Earth System Science, Tsinghua University, Beijing 100084, China

J. He · Y. Wang (✉) · J. Hao · L. Shen · L. Wang
School of Environment, Tsinghua University, Beijing 100084, China
e-mail: yxw@mail.tsinghua.edu.cn

Introduction

Ozone is produced in the troposphere by photochemical reactions of nitrogen oxides (NO_x), carbon monoxide (CO), and volatile organic carbons (VOCs). High ozone near the surface has an adverse impact on human health and vegetation (NCR 1991) and is thought to be responsible for crop damages (Cheung and Wang 2001; Pochanart et al. 2003). Consumption of fossil energy especially coal (NBS 2007) and increasing vehicular emissions (Hao and Wang 2005) result in large increases in ozone precursor emissions in China with implication for tropospheric chemistry. Great efforts have been made to obtain in situ measurements of surface ozone in China (Wang et al. 2001, 2002, 2004, 2005, 2006; Gao et al. 2005; Lin et al. 2008; Ding et al. 2008; Wang et al. 2010). The in situ measurements suggested that surface ozone was relatively low in summer at rural and coastal sites over east China, ranging from Hong Kong (Wang et al. 2005), to Shanghai (Wang et al. 2004), to Beijing (Lin et al. 2008; Wang et al. 2006), in contrast to the pattern observed typically in North America and Europe (maxima in summer).

Previous studies have suggested that the East Asian summer monsoon (EASM) has significant influences on the seasonal variation of ozone in East Asia (Luo et al. 2000; Yamaji et al. 2006; Li et al. 2007; Wang et al. 2008, 2011). The temporal and spatial distribution of tropospheric ozone is strongly related to meteorological condition and atmospheric circulation. In summer, the weather of east China is under the control of the EASM. Its clean maritime inflow with lower ozone background and precursors contributes to the relatively low surface ozone in summer (Wang et al. 2011).

In order to further study the variability in surface O_3 and its association with EASM over the Yangtze River Delta (YRD) region in central east China, Tsinghua University founded an ozone observation station at the Chongming Island to the

northeast of Shanghai. The site was selected to capture the dichotomy between relatively clean maritime air and polluted continental air with the urban plume from Shanghai and other cities in the YRD. Shanghai is one of the most rapidly developing metropolises in China with a population of over 20 million. It faces serious air pollution problems due to population growth, economic expansion, and industrial development in recent years. Better understanding of the relevant physics and chemistry of O_3 can play a significant role in finding cost-effective measures to reduce ozone pollution. The purpose of this study is to understand the effect and the mechanism of the EASM on surface ozone variability at Chongming in summertime based on in-depth analysis of measurements during August 2010. The association of O_3 and meteorological parameters will be used to develop an understanding of weather patterns influencing variations of O_3 over the YRD region in August. A chemical transport model is adopted to test the mechanism and to separate the effects of local emissions and meteorology.

Site description and general meteorology

Site description

The Chongming site (31°31′ N, 121°54′ E, 24 m a.s.l.) is located in the eastern part of the Chongming Island. The Island is in the mouth of the Yangtze River, about 30 km northwest to Shanghai urban center. The Yangtze River flows between the Island and Shanghai urban area before reaching the Yellow Sea (Fig. 1). The eastern part of the Island is mostly wetland and designated protection areas for migrating birds, covered mostly by trees and bushes with no major pollution sources. Located near Shanghai and to the east of the developed YRD region, the Chongming site is an optimal place to measure the chemical characteristics of outflow from east China and the contrast between east China outflow and the maritime inflow.

The measurements of tracer gases (O_3, CO) and basic meteorological data (wind speed and direction, temperature, relative humidity, pressure, and solar radiation) began in May 2009. Surface ozone is measured using an analyzer based on UV absorption (Thermo Environmental Instruments Model 49c). CO is measured using an analyzer based on infrared absorption (Thermo Environmental Instruments 48CTL). The instruments are kept in a room on the top floor of a three-floor building at a height of 24 m above the ground level, with a 5-m long Teflon inlet shared by the two instruments. There is a particulate filter in the inlet to prevent particles from entering the instruments. Sample air is drawn from the inlet and is dried by a cold trap held at 2 °C and Nafion drier continuously. Exhaust air from the instruments is used to purge the Nafion drier before venting to the room. Raw data are recorded by the instruments at a frequency of 1 min. In order to keep the measurement accuracy, quality analysis and quality control are performed periodically. Instrument zero of CO is determined by diverting sample air through an oxidizing catalyst to remove CO (Foulger and Simmonds 1993) for 3 min every 15 min. Twice daily, the instrument gain is determined by supplying NIST traceable standards (Scott-Marrin). The ozone instrument is calibrated with a UV photometric primary standard (Thermo Environmental Instruments 49i-PS) every 6 months. For the purpose of studying day to day and diurnal variations of ozone in the present study, we use hourly mean observation data at the site.

East Asian summer monsoon and Western North Pacific subtropical high

East China is in the East Asian monsoon domain. Southerly wind prevails in summer and northerly wind in winter. The climatological dates of the onset of the EASM is from the first to second dekad of June characterizing the arrival of the East Asian rainy season such as the Meiyu over the Yangtze River Basin (Ding et al. 2004). The seasonal advance and retreat of the EASM behave in a stepwise way. It undergoes three stationary periods and two abrupt northward jumps (Ding and Johnny 2005). These stepwise northward jumps are closely related to seasonal changes in the general circulation in East Asia, in coincidence with the westward and northward

Fig. 1 The location of Chongming site (*red dot*). The *red rectangle* indicates the Yangtze River Delta (YRD) region

expansion of Western Pacific subtropical high (WPSH), which is one of the most important components of the East Asian monsoon (Tao and Chen 1987). With the development of EASM, WPSH expands westward, while it moves or jumps northerly. In summer, the ridge of WPSH expands northwest, influencing the weather patterns of east China (Huang and Yu 1962; Tao and Zhu 1964; Chang et al. 2000; Liu and Wu 2000). In August, the ridge moves to the vicinity of 30°N and the Chongming site is under the control of descending currents under the ridge of the WPSH. The weather is clear and hot, implying the favorable conditions for photochemical production of ozone in the daytime.

A very strong WPSH occurred in summer 2010 over East China with its ridge north of 32°N (NCC/CMA). This means a typical weather pattern with higher temperature and lower relative humidity in the lower troposphere favorable for local ozone production over the YRD. In order to investigate the influence of the WPSH on surface ozone over East China, the present study focuses on measurements of O_3 and CO at Chongming in August 2010.

Model description

We used the nested-grid GEOS-Chem chemical transport model developed by Wang et al. (2004) and Chen et al. (2009) to simulate surface ozone observations at Chongming. The purpose of using a chemical transport model with assimilated meteorology is to separate the role of meteorology and emissions on the variability of ozone at Chongming. The model is driven by meteorological data assimilated by the Goddard Earth Observing System (GEOS-5) at the NASA Global Modeling and Assimilation Office. We use GEOS-Chem model version v8-02-01 with a horizontal resolution of 0.5° latitude by 0.667° longitude over the nested domain (70°E–150°E and 11°S–55°N, includes all of China, parts of neighboring countries, and a significant portion of the northwestern Pacific) and 47 vertical hybrid eta levels, extending from the surface to 0.01 hPa.

The GEOS-Chem model includes a detailed tropospheric simulation of the complex chemical interactions between ozone, nitrogen oxides (NO_x), hydrocarbons, and aerosols. The model uses the advection algorithm of Lin and Rood (1996), consistent with the meteorological simulation in the GEOS GCM. Convective transport in GEOS-Chem is computed from the convective mass fluxes in the meteorological archive. Anthropogenic emissions of ozone precursors over China were adopted from the inventory of Zhang et al. (2009) for 2006. Application and evaluation of the nested-grid GEOS-Chem model over China has been described in detail by Wang et al. (2004a,c, 2011). The atmospheric life of ozone is 1–2 weeks in summer and 1–2 months in winter and atmospheric life of CO is 1–2 months on average. To remove the influence of initial conditions, the model was spin-up for months from May 2010 and then run through the end of August 2010. Hourly model output sampled at the grid box that includes Chongming is used for comparison with observations.

Results

Day to day variations

Figure 2a presents the hourly mixing ratio of ozone observed at Chongming in August 2010. The mean mixing ratio of ozone in August is rather low (34 ppb), but there are large day-to-day

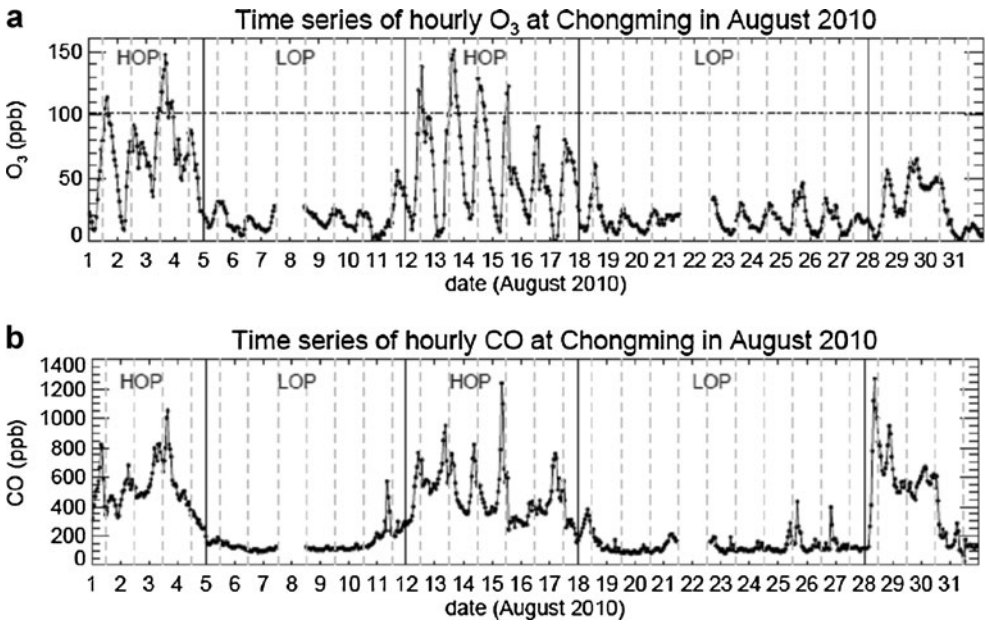

Fig. 2 Time series of hourly O_3 (**a**) and CO (**b**) mixing ratios at Chongming in August 2010. The *dash lines* indicate the noon of day, and the *dotted line* indicates the102 ppb of O_3. HOP and LOP are indicated by the *vertical lines*

variations (standard deviation of 30 ppbv). At night, the ozone levels are generally below 20 ppb except for the dates of 3–4 August and 29–30 August, as a result of inactive photochemistry and reduced boundary layer height. First, reduced vertical mixing and depth of the boundary layer at night allow enhanced depletion of ozone at the surface while it suppress transport of ozone from aloft. Second, mixing ratios of freshly emitted NO increase at night because of reduced vertical mixing and no photolysis loss, resulting in enhanced titration effect of NO on O_3 ($NO+O_3 \rightarrow NO_2+O_2$). In the daytime, the ozone levels have a large range from 20 to 150 ppb. The diurnal variation of ozone is considerably large during the periods of 1–4 August and 12–18 August.

Figure 2b presents hourly mixing ratios of CO observed at Chongming in August 2010. The mean daytime mixing ratio of CO is 330 ppb±250 ppbv, relatively lower compared with other surface sites in China such as Miyun, a rural site about 100 km northeast of Beijing (500 ppb in August 2006) (Wang et al. 2008). Similar to ozone, the day-to-day variations of CO are large, ranging from 100 to 1000 ppb. During the periods of 1–4 and 12–18 August when ozone levels are high, CO levels are higher than other days.

Table 1 lists the days and the number of hours with 1-h mean mixing ratios of ozone exceeding 102 ppb (China's ambient air quality standard for ozone at 1 atm and 25 °C). There are two distinct periods of high ozone period: 1–4 August and 12–18 August. In the first period, there are 14 h when the ozone mixing ratios exceed the air quality standard, noting that the lowest values of ozone mixing ratios over the days of 3–4 August are above 35 ppb. In the second period, the number of hours with ozone exceeding the standard is 19 h with lowest values of ozone mixing ratios below 20 ppb. We define the dates of 1–4, 12–18 August as the high ozone periods (HOP) that have the mean daytime mixing ratios of 92 ppb. In contrast, ozone levels on 5–11 and 19–28 August are significantly lower, with daytime mean mixing ratios of only 21 ppb. We define these days as the low ozone periods (LOPs).

Comparing Fig. 2a and b, we can see that the day-to-day variability of CO is similar to that of ozone. The correlation of CO and ozone has been used in many researches to examine the effects of anthropogenic precursors on ozone (Chin et al. 1994; Parrish et al. 1998; Mao and Talbot 2004).

Table 1 The numbers of hours with 1-h mean concentrations of O_3 exceeding 102 ppb (Chinese air quality standard for ozone) in August

Date	Hours (O_3>102 ppb)
1	3
3	11
12	4
13	7
14	6
15	2

Figure 3 presents the different correlations between hourly daytime CO and ozone observed at Chongming during HOP and LOP. The coefficient of correlation is 0.75 during HOP, decreasing to 0.52 during LOP. The stronger O_3–CO correlation during HOP indicates the influences of anthropogenic precursors on the production of ozone. Higher CO observed at Chongming site also indicates the air masses during HOP were mainly from the urban areas. The O_3–CO correlation slope is 0.13–0.15 ppb ppb^{-1}, smaller than those in North American (0.3–0.4 ppb ppb^{-1}) (Mauzerall et al. 2000; Pochanart et al. 2003), in consistence with the study by Wang et al. (2006) in a rural area of Beijing.

Figure 4 presents hourly time series of temperature (Fig. 4a), RH (Fig. 4b), and surface pressure (Fig. 4c) observed at Chongming in August 2010. During HOP defined above, both daytime and nighttime temperatures are higher than that in other days. The maximum temperature is 37 °C on 14–15 August. The RH at noon is much lower during HOP than during other days. The minimum RH is 60 % on 14–15 August compared with the typical value of 80 % on other days. There is an alternative pattern of low and high pressures that can last for a few days each (Fig. 4c). Surface pressure is relatively lower during HOP. We will show the association of HOP and LOP with different weather patterns controlled by the continental and marine air masses, respectively.

Diurnal cycles

Figure 5 presents the mean diurnal cycles of O_3 (Fig. 5a), CO (Fig. 5b), temperature (Fig. 5c), RH (Fig. 5d), surface pressure (Fig. 5e), solar radiation (Fig. 5f), and wind speed (Fig. 5g), respectively, averaged during HOP and LOP. During HOP, ozone shows large diurnal changes. The lowest value (<20 ppb) and highest value (>100 ppb) occur at 5–6 A.M.

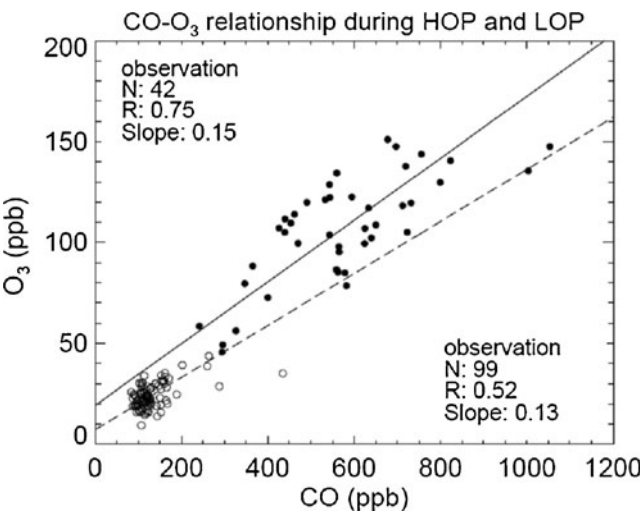

Fig. 3 The CO–O_3 relationship observed at Chongming during HOP and LOP in August 2010. The *filled circle* and *solid line* are for HOP, and the *open circle* and *dashed line* are for LOP

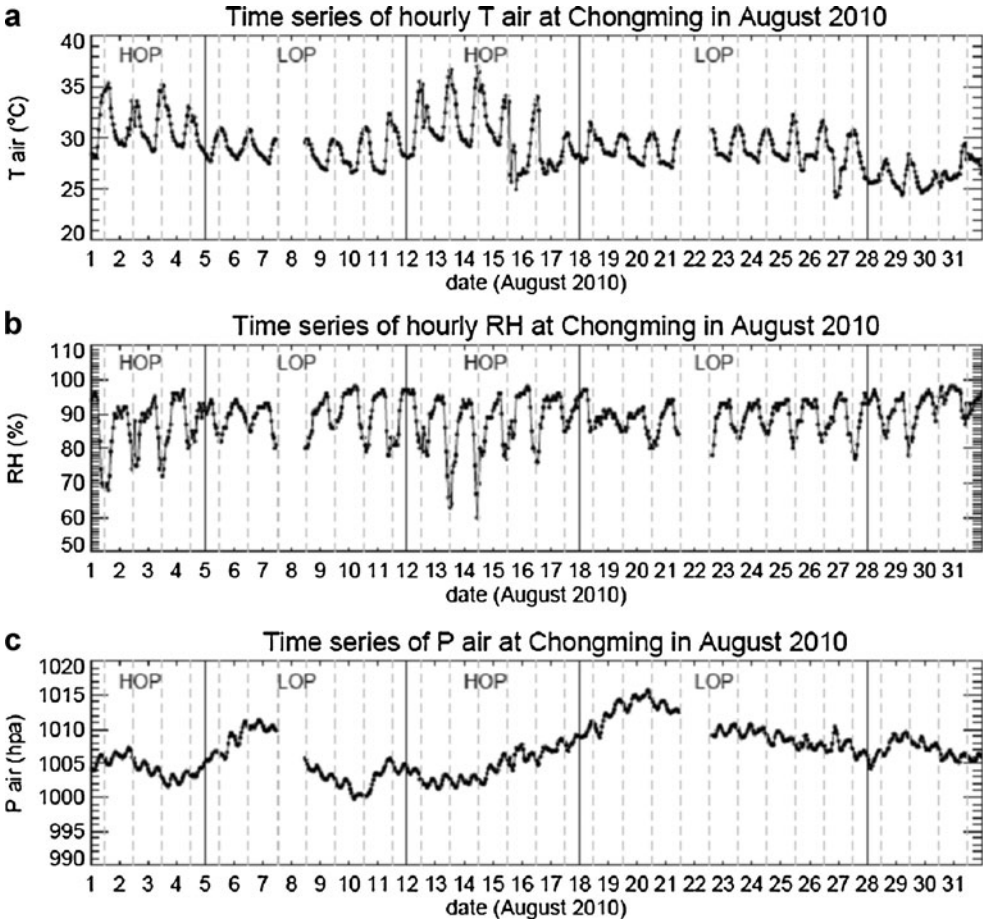

Fig. 4 Time series of air temperature (**a**), RH (**b**), and surface pressure (**c**) at Chongming in August 2010. The *dashed lines* indicate the noon of day. The HOP and LOP are indicated by the *vertical lines*

and 1 P.M., respectively. The diurnal cycle of CO is different from that of O_3. It increases gradually from midnight and peaks at 8 A.M. with the highest value of 750 ppb, then it decreases gradually in the daytime and reaches the lowest value of 400 ppb at 8 P.M. and, afterwards, keeps nearly a constant level to midnight. During LOP, the diurnal change in O_3 is much smaller with low value of ozone mixing ratios in the nighttime (about 10 ppb) and a gradual increase in the daytime (about 20 ppb). CO stays almost constant throughout the day at a level of 150 ppb or so.

Temperature and RH shows large diurnal cycle with higher temperature and lower RH in the daytime, while the diurnal change of surface pressure is relatively small. Temperature has a similar trend to that of solar radiation in the day except that the peak time is different. Temperature peaks at noon and ozone peaks 1 h later than temperature. This is different from the measurements at a rural site near Beijing (Miyun) where ozone peaks at 4 P.M. (Wang et al. 2010). It is mainly because the two sites are in different latitudes with different weather systems and emissions. The mean peaking temperature at noon during HOP is about 4 °C higher than that during LOP. The difference in RH between HOP and LOP occurs mainly in the daytime. Corresponding to the temperature maximum, the minimum of RH occurs at 11 A.M. The diurnal change of pressure is similar during HOP and LOP, with higher pressure in the morning and lower pressure in the afternoon. Surface pressure throughout the day during HOP is about 4 hPa lower than that during LOP. The peak solar radiation in HOP is slightly smaller than that in LOP. The diurnal change of wind speed is similar during HOP and LOP, with stronger wind in the daytime. During HOP, the maximum wind speed (4 m/s) occurred at 12 P.M. and minimum wind speed at 5 A.M. and 8 P.M., respectively. During LOP, the maximum wind speed (2 m/s) occurred at 1 P.M. and minimum wind speed at 5 A.M. The wind speed throughout the day during LOP is about 1–2 m/s higher than that during LOP except at 7 and 8 P.M. (<0.5 m/s). The diurnal change in wind speed is associated with thermodynamic circulation near the surface.

Wind

Wind is a key factor to indicate transport patterns. Figure 6 presents the wind rises during HOP and LOP. Winds are mostly southerly during both HOP and LOP, indicating that under the influence of the EASM, the ridge of the WPSH has moved to the vicinity of Chongming in August. However, during HOP, about 40 % of the time the winds are from N–NNW–NW, indicating the influence of continental outflow at the site. During LOP, ESE–SE–SSE–S

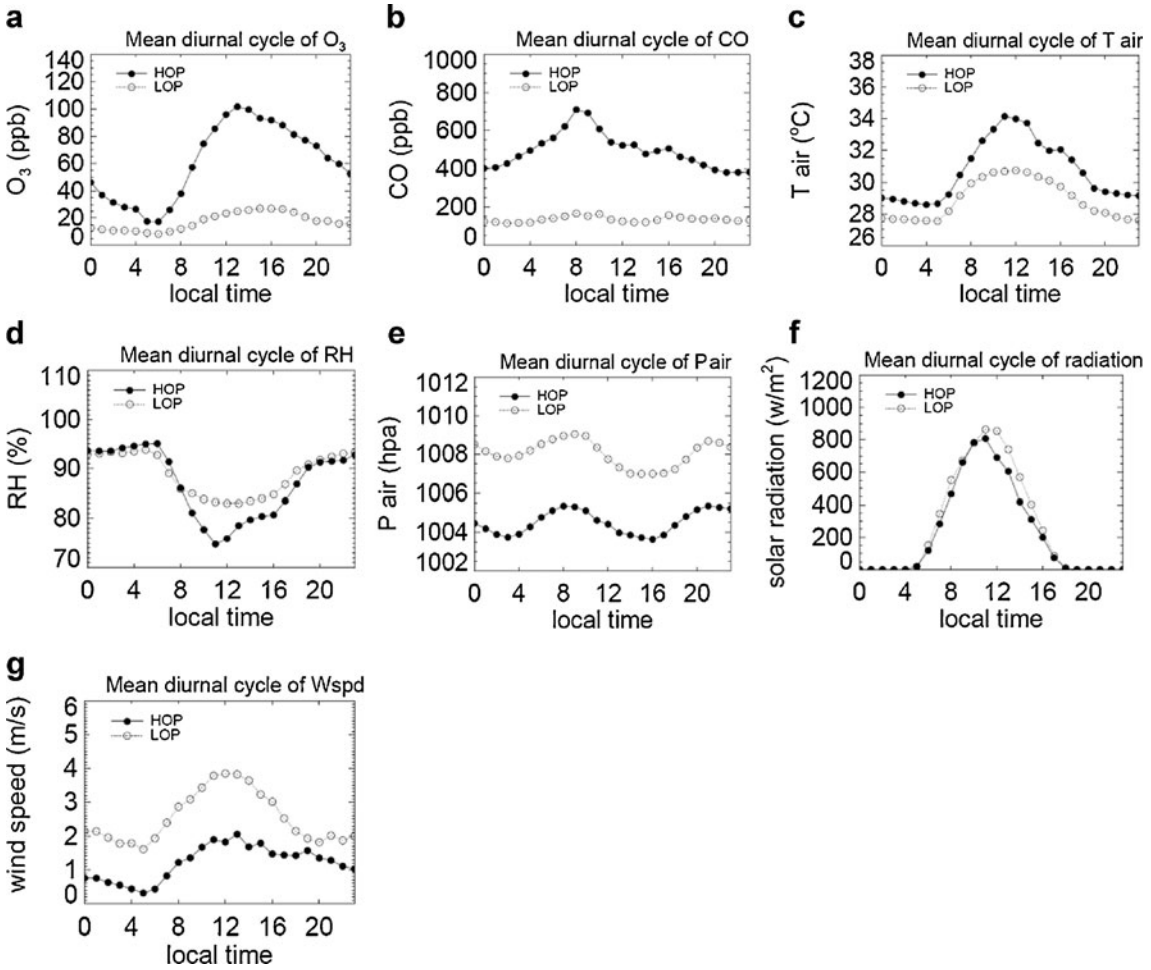

Fig. 5 Mean diurnal cycles of O_3 (**a**), CO (**b**), air temperature (**c**), RH (**d**), surface pressure (**e**), solar radiation (**f**), and wind speed (**g**) at Chongming during HOP and LOP in August 2010. The *filled circle* and *solid line* are for HOP and the *open circle* and *dashed line* are for LOP

winds are more frequent indicating the marine air inflow. Although southerly wind blows >40 % of the time during HOP and LOP, wind speed is quite different. During HOP, the mean southerly wind speed is <1.4 m/s, while during LOP, it is a factor of 2 higher, >2.8 m/s. The median southerly wind speed has the same variations as the mean speed between HOP and LOP. Smaller wind speed is favorable for the local photochemical production and accumulation of ozone.

In this section, we show that although the monthly mean ozone mixing ratio is relatively low (34 ppb) at Chongming in August, there are large day-to-day variations of ozone with noticeable high ozone periods that typically last for 3–5 days with daily peaking ozone levels exceeding 102 ppb and low ozone periods with daily peaking ozone levels lower than 20 ppb. CO levels are much higher during HOP than those during LOP, indicating that HOP are of anthropogenic origin. Ozone and CO exhibited large diurnal variations during HOP, while the diurnal variations of both species became much flatter during LOP. The meteorological conditions are found to be different. During HOP, northwesterly winds are more frequent, indicating the influence of continental pollution. At the same time, wind speed is small, suggesting a stable meteorological condition for accumulation of pollution plumes.

Discussion

Temporal correlation between ozone and meteorological factors

The meteorological factors are closely associated with weather patterns. Analyzing the correlations of ozone and meteorological factors will contribute to deeper understanding of the influences of weather patterns on ozone variations. Figure 7 presents the correlation between daily maximum ozone and selected meteorological factors: daily maximum temperature (Fig. 7a), daily range of RH (Fig. 7b), and daily mean surface pressure (Fig. 7c). The correlation coefficients between daily maximum ozone and daily maximum temperature, daily range

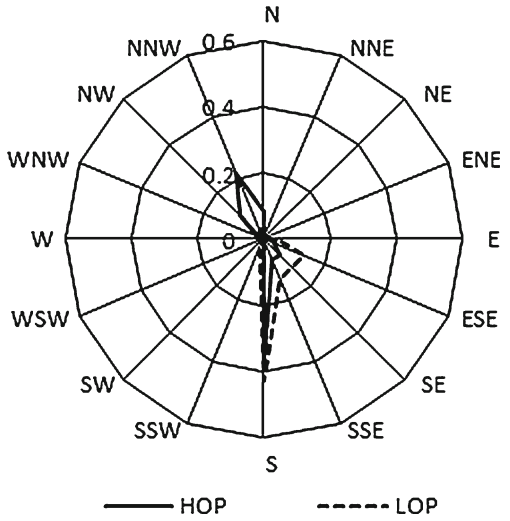

Fig. 6 Wind rose of wind directions at Chongming for HOP and LOP. The ratio indicates the frequency of wind observed in each direction

of RH, and daily mean surface pressure are 0.8, 0.78, and −0.54 respectively. Temperature is a key factor in determining the reaction rates of key chemical reactions critical to the ozone variations (Jacob et al. 1993; Xu et al. 2011). The strong positive correlation between ozone and temperature is consistent with general understanding of ozone chemistry and dynamics that have been well documented by observations worldwide (NRC 1991; Steiner et al. 2010; Xu et al. 2011). Previous studies suggested that ozone would have a negative correlation with RH due to the reaction of ozone with water vapor (Davis and Speckman 1999; Elminir 2005), as RH indicates water vapor content in the air. As RH is typically lower in the day than that at night, the diurnal range of RH becomes larger when daytime RH decreases. Therefore, the strong positive correlation between daily maximum ozone and the daily range of RH at Chongming is an alternative way to show the negative correlation with ozone and daytime RH.

We find that the daily range of RH has a stronger correlation with daily maximum ozone than the daytime RH does. The reason is that the daily range of RH better reflects the weather patterns resulting in ozone production. The larger daily range of RH and higher daily maximum temperature indicate that the weather is under the control of WPSH with clear sky, which features lower temperature and higher RH at night. At noon, temperature rises rapidly, while RH decreases sharply, resulting in higher daily maximum of temperature and lower RH, favorable for ozone production. This implies that the daily range of RH is a better factor than daytime RH to predict maximum daytime ozone level over the YRD region in summer.

Previous studies have found that high ozone pollution events occurred preferably during high pressure conditions (Hanna 1991; Xu et al. 1997, 2011; Eshel and Bernstein 2006). Wild et al. (2004), using a global chemical transport model, suggested that the high pressure conduced to strong ozone production over East Asia by keeping ozone and precursors within the boundary layer. The negative correlation exhibited between ozone and surface pressure at Chongming under the control of WPSH appears to be in contrary to this general understanding. As WPSH is the prevailing weather system over YRD in summer, surface pressure change is associated with the change in the location and intensity of WPSH, rather than driven by the shifts between transient high and low pressure regimes. Therefore, the negative correlation between surface ozone and surface pressure indicates the effects of WSPH variation on ozone. An analysis of the vertical variation of O_3 and related meteorological factors is conducted next to further investigate the mechanism.

Vertical variation of O_3 and related meteorological factors

As we do not have in situ measurements of vertical profiles of ozone and meteorological factors, the vertical distributions of ozone and meteorological factors from the GEOS-Chem model are used to further analyze the impact of WSPH on ozone at Chongming. We first evaluate the model's performance in simulating surface-level ozone and meteorological fields at Chongming by comparing model results with observations (Fig. 8). The model well captures

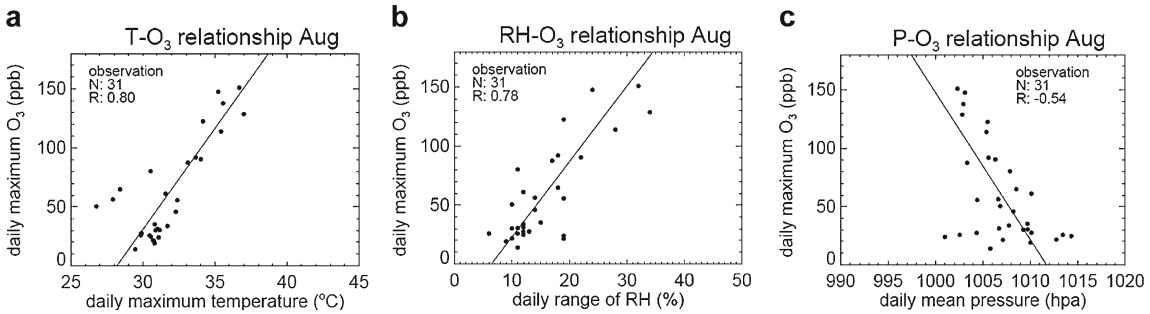

Fig. 7 **a** The relationship between daily maximum ozone (*y*-axis) and daily maximum temperature (*x*-axis) observed at Chongming in August 2010. Each point refers to daily mean mixing ratios. Correlation coefficients (*R*) are shown in *inset*; **b** same as **a**, but for the daily range of RH (*x*-axis); **c** same as **a**, but for daily mean pressure (*x*-axis)

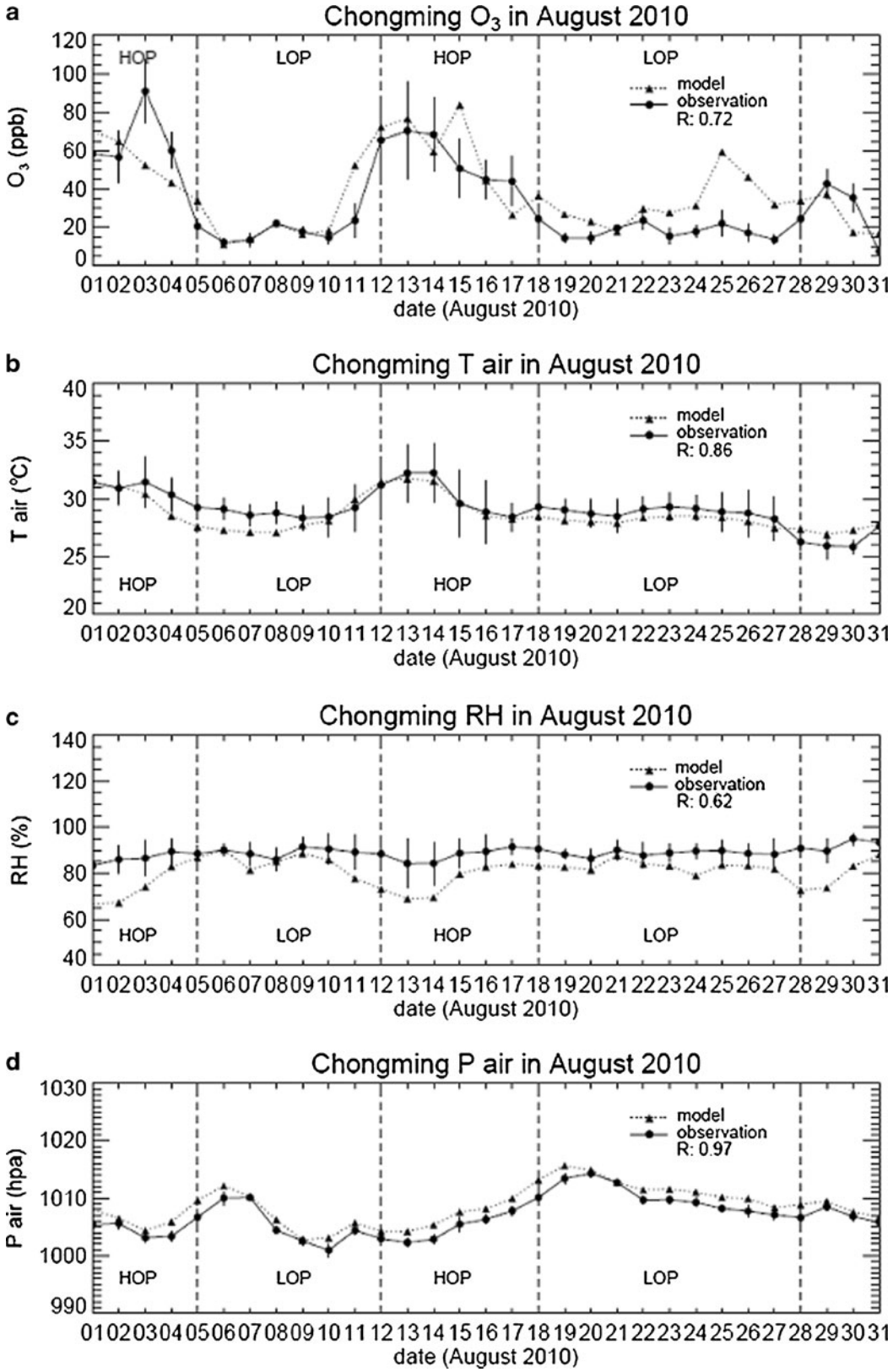

Fig. 8 Comparisons of observed and modeled day-to-day variations in surface ozone (**a**), air temperature (**b**), RH (**c**), and surface pressure (**d**). Observations are indicated in *solid lines* and the GEOS-Chem model results in *dotted lines*

the concentration levels and variations in surface O_3 at Chongming, with the correlation coefficient with observations of 0.72 and a mean positive bias of 3 ppbv. The GEOS-5 assimilated meteorological fields used to drive the model match well with observations, including temperature, RH, and surface pressure, which are critical meteorological factors affecting O_3 production. RH in the model is generally 5–10 % lower than observations.

In Fig. 9, we compare the daily (24 h) mean vertical profiles of O_3 (Fig. 9a), temperature (Fig. 9b), and RH (Fig. 9c) between HOP and LOP obtained from the GEOS-Chem model. As illustrated in Fig. 9a, the vertical variation in O_3 during HOP is quite different from that during LOP. During LOP, the mean ozone mixing ratio increases from about 20 ppb at 70 m (the lowest model level) to 25 ppb at 200 m, then increases slowly with altitude to 30 ppb at 2,000 m. During HOP, the mean ozone mixing ratio increases rapidly from about 60 ppb at 70 m to 80 ppb at 200 m and increases further to 87 ppb at 500 m, then gradually decreases to 37 ppb at 1800 m with little changes upwards. This vertical profile of O_3 is associated with the vertical profile of temperature (Fig. 9b). The temperature in the boundary layer in HOP is about 2–5 °C higher than that in LOP. The difference in temperature between HOP and LOP is larger at the surface than in the middle and upper boundary layer. In particular, temperature increases with height below 200 m during HOP.

The vertical profile of temperature is closely associated with subsidence inversion caused by the subsidence flow under the ridge of WPSH. When the intensity of WPSH decreases, the subsidence flow become weaker and cannot penetrate to the surface, resulting in a buildup of an isothermal or inversion layer near the surface. The inversion layer suppresses vertical motions and weakens the subsidence flow in the middle and low level of WPSH. As a result of relatively high temperature in the inversion layer, air density decreases, resulting in reductions of surface pressure and further decreases in the intensity of WPSH. This corresponds to the temperature profile during HOP and explains the negative correlation between ozone and surface pressure. On the other hand, during LOP, the subsidence flow associated with a stronger WPSH bring free tropospheric air all the way down to the surface. As temperature increases during the subsidence, there is no inversion layer at the surface. Corresponding to the vertical variation of temperature, the mean RH (Fig. 9c) during HOP decrease rapidly from 72 % at 70 m to 60 % at 330 m and remains more or less constant till 500 m, then gradually increases to 72 % at 1,200 m and remains little changes upwards. The mean RH during LOP is higher than that during HOP, and it gradually decreases from 85 % at 70 m to 70 % at 2,000 m. The differences of vertical profiles for temperature and RH between HOP and LOP suggest that the inversion layer near the surface as a result of subsidence flow associated with the intensity of WPSH is conducive to pollutant accumulation and photochemical production of ozone.

Circulation patterns

Figure 10 presents observed pentadly mean 850 hPa wind fields in August 2010 for the large geographical regions influenced by EASM (NCC/CMA 2010). The first and third pentad corresponds approximately to HOP while the second and fourth pentad to LOP. The red dot on the figure indicates the Chongming site, and the green box indicates the South China Sea region with significant influences on EASM. Winds in the low troposphere prevail southwesterly over Chongming during HOP, compared to southeasterly during LOP. Over the South China Sea, winds are strong southerly and southwesterly respectively during HOP and LOP. Figure 11 presents the mean wind fields at the surface overlaid with surface ozone (Fig. 11a, b), air pressure (Fig. 11c, d), and air temperature (Fig. 11e, f) from the GEOS-Chem model averaged during HOP and LOP, respectively. During HOP (left panels of Fig. 11), the center of WPSH is to the southeast of the YRD region (Fig. 11c). The region is predominated by SW winds with smaller wind speed, lower surface pressure, and higher temperature, which are favorable for high ozone episodes. During LOP (right panels of Fig. 11), the center of WPSH is to the northeast of YRD region (Fig. 11d). The region is controlled by SE winds with stronger wind speed, higher pressure, and lower temperature. The EASM transports maritime air with less abundance of

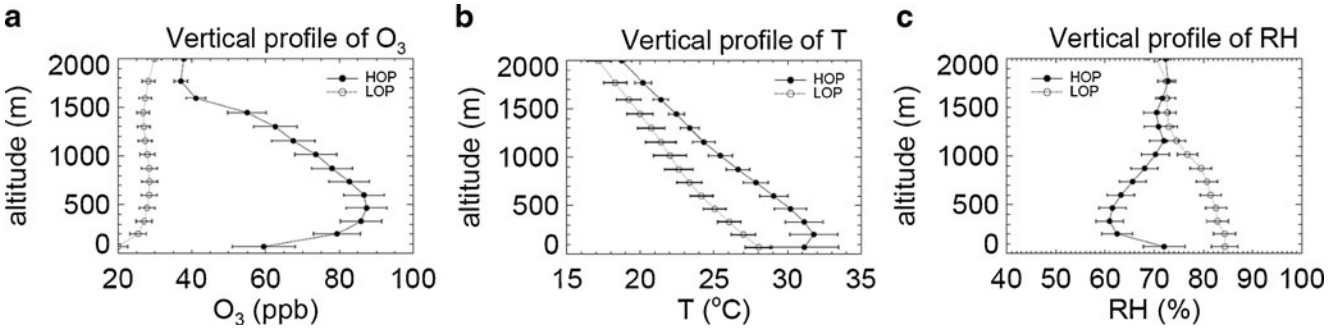

Fig. 9 Mean vertical profiles of O_3 (**a**), air temperature (**b**), and RH (**c**) at Chongming during HOP and LOP in August 2010. *Solid lines* are for HOP and *dotted lines* for LOP

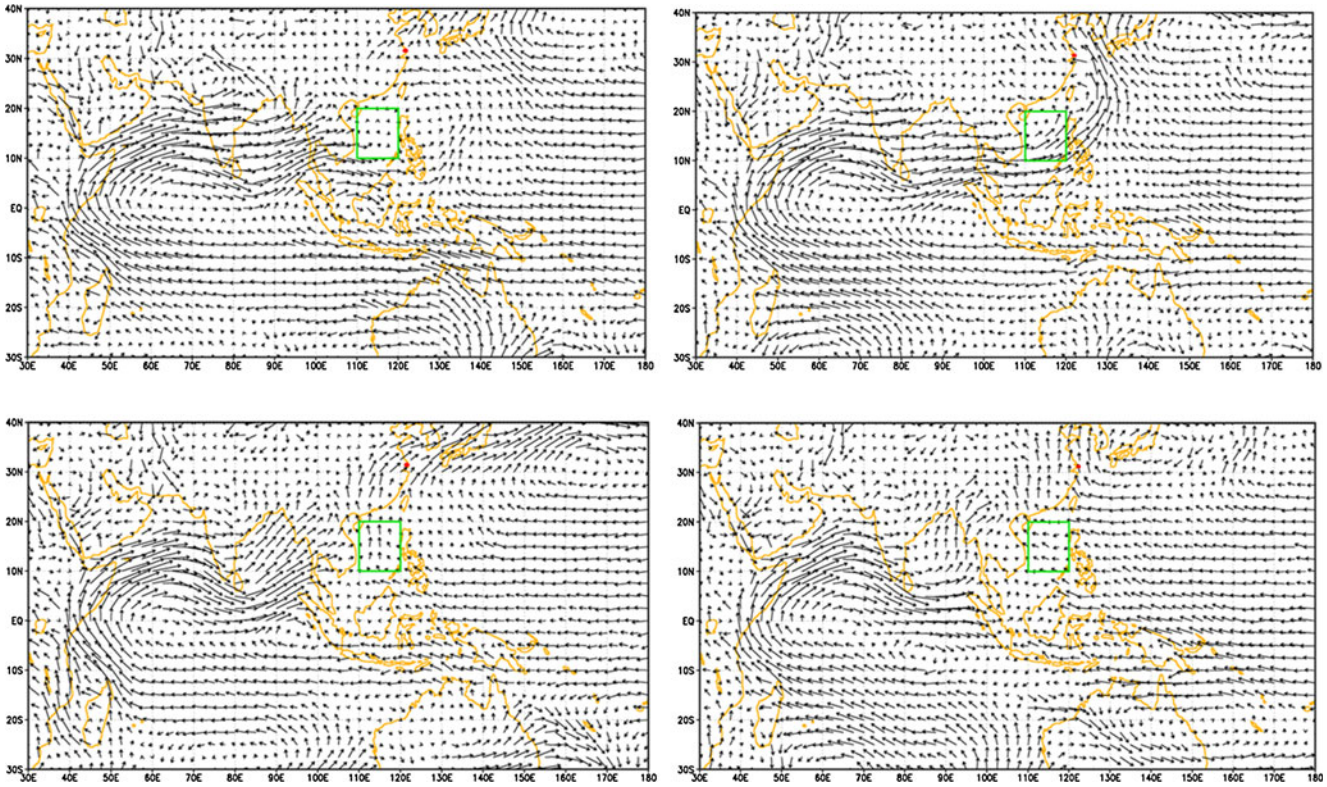

Fig. 10 Pentadly mean 850 hPa wind fields (NCC/CMA) for 1–5 August (*upper left*), 6–10 August (*upper right*), 11–15 August (*bottom left*), and 16–20 August (*bottom right*), 2010. *Red point* indicates the Chongming site. *Green box* indicates the South China Sea monsoon monitoring area

ozone and ozone precursors. The inflow of clean marine air results in less ozone production at the site. The intensity of WPSH is coincident with surface pressure change at Chongming. During HOP mean surface pressure at Chongming is about 6 hPa lower than that during LOP, resulting in the negative correlation between ozone and surface pressure presented before.

Influence of emissions

In order to separate the influence of anthropogenic emissions on ozone variability, a sensitivity simulation was conducted in which anthropogenic emissions of ozone precursors (NO_x, VOCs, and CO) from the YRD region were zeroed out in the GEOS-Chem model. The day-to-day variations of O_3 and CO at Chongming site from the standard and sensitivity simulation were compared in Fig. 12a and b, respectively. During HOP, the mean mixing ratios of O_3 and CO are reduced by 36 and 246 ppbv, respectively, in the sensitivity simulation compared to the standard simulation. During LOP, the reductions are much smaller, about 4 ppbv for O_3 and 56 ppbv for CO. The difference in model results indicates that anthropogenic emissions in YRD contribute to 52 % of surface ozone concentrations during HOP, whereas their contribution reduces to only 15 % during LOP. Given that anthropogenic emissions do not change from LOP to HOP, the different contributions of emissions to ozone between LOP and HOP suggests that surface ozone at Chongming in August is very sensitive to meteorological conditions associated with the variability of WPSH. When the center of WPSH is to the southeast of Chongming site with reduced intensity and weaker subsidence, which is the meteorological conditions during HOP, it is conducive for accumulation of anthropogenic emissions in YRD and for production and accumulation of O_3. On the other hand, during LOP, stronger WSPH located to the northeast of Chongming with southeasterly winds and stronger subsidence results in efficient dispersion of local anthropogenic emissions. Therefore, local anthropogenic emissions make significant contributions to surface ozone concentrations only during HOP.

In August, the weather in east China is under the control of WPSH. The weather conditions during HOP are quite different from that during LOP. On one hand, the vertical profiles of temperature and RH are different. During HOP, the inversion or isothermal layer (below 500 m) at Chongming results in the weather pattern characterized by higher temperature and lower RH. During LOP no inversion or isothermal layer occurs and the weather pattern is characterized by lower temperature and higher RH. The inversion or isothermal layer results in trapping of pollutants such as anthropogenic emissions including ozone precursors

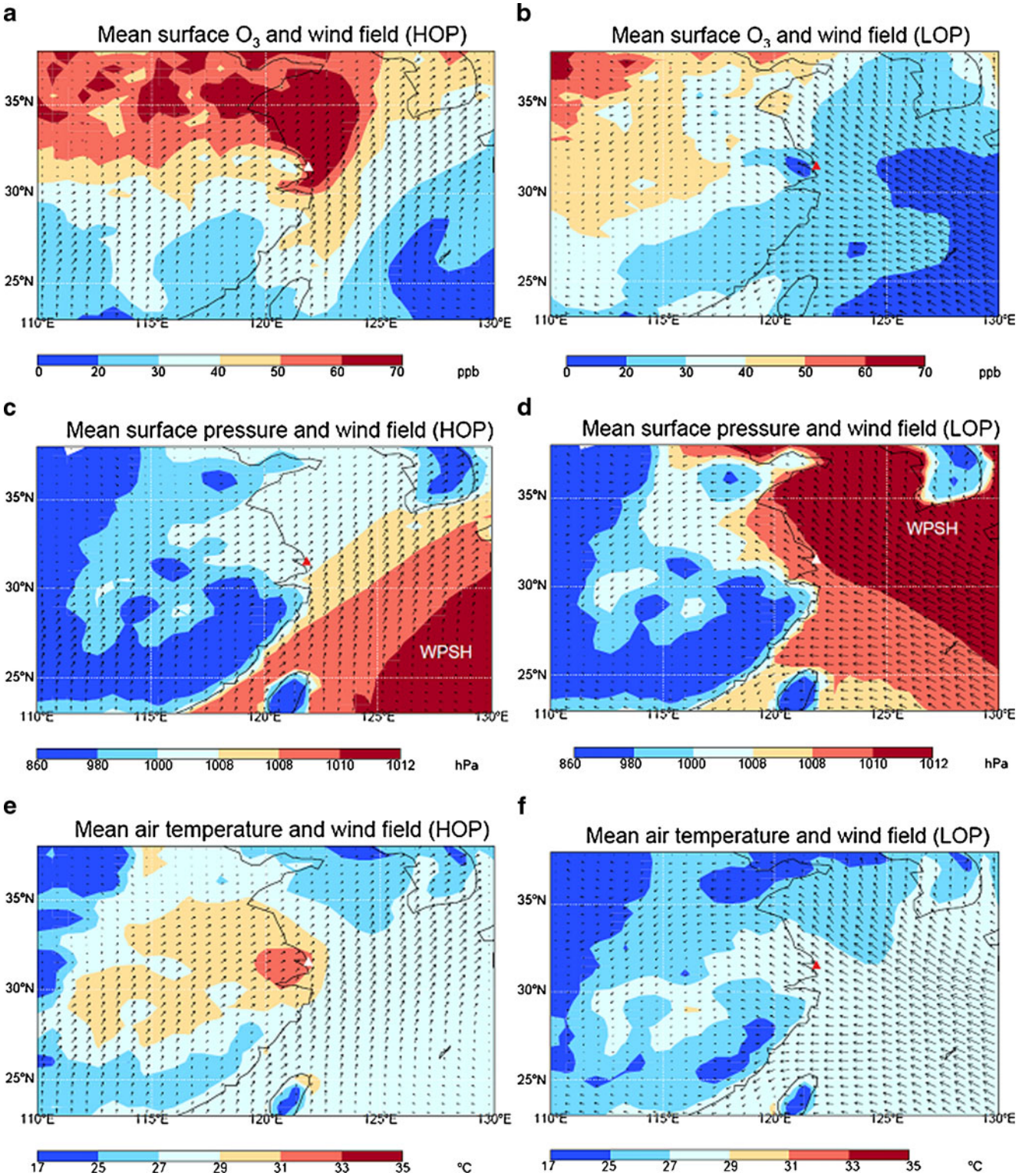

Fig. 11 Mean wind fields atop the filled contour plots of surface O_3 (**a**, **b**), surface pressure (**c**, **d**), and air temperature (**e**, **f**) in August 2010. The *left panels* are mean model fields during the HOP, and the *right panels* are for LOP. *White* or *red triangle* indicates the Chongming site

close to the ground and suppresses vertical mixing by making the surface air more stable. On the other hand, the circulation patterns are different. The weaker SW winds with aged urban pollution and stronger SE wind with clean maritime air prevail during HOP and LOP respectively. During HOP, the stagnant condition is favorable for ozone

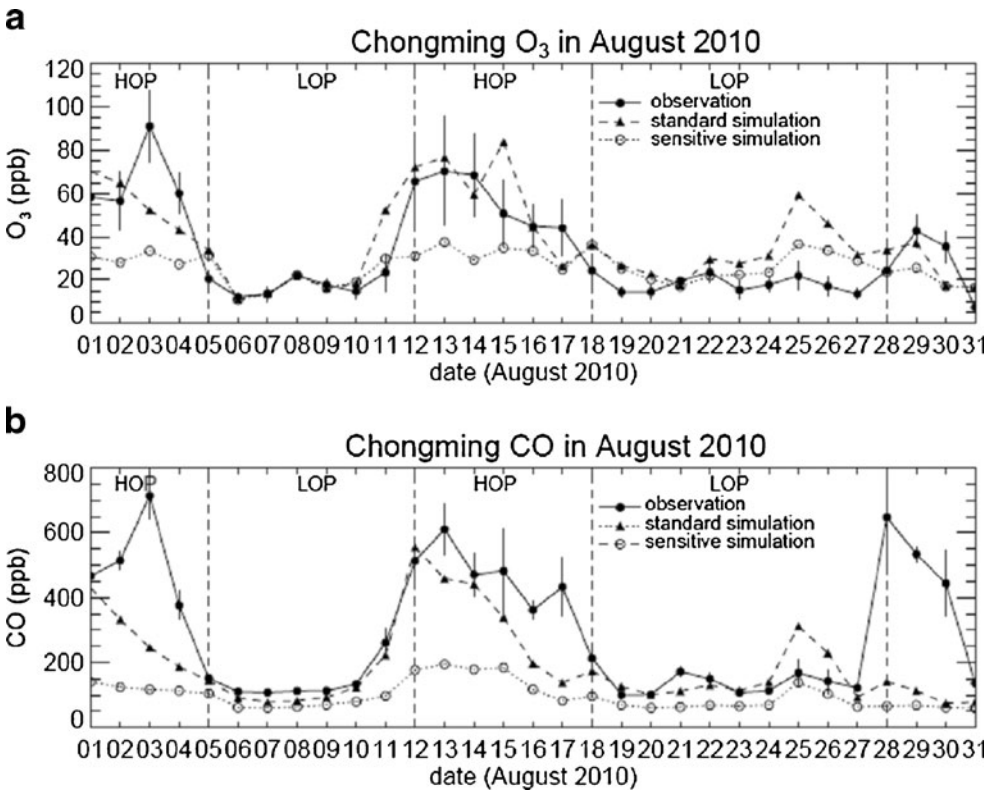

Fig. 12 Comparisons of observed and modeled day-to-day variations in surface ozone (**a**) and CO (**b**). Observations are indicated in *solid lines* and the GEOS-Chem model results in *dash lines* (standard simulation) and *dotted lines* (sensitive simulation)

production and accumulation of ozone precursors and ozone. Model sensitivity simulation suggests that surface ozone at Chongming in August is very sensitive to meteorological conditions. Local anthropogenic emissions make significant contributions to surface ozone concentrations only during HOP when the center of WPSH is to the southeast of Chongming with reduced intensity and weaker subsidence.

Concluding remarks

In summer, with the development of the summer monsoon, WPSH moves northwesterly and increases in intensity. In August, the ridge of WPSH moves to the vicinity of 30°N above the YRD region. We find that ozone mixing ratios at Chongming in August 2010 are strongly correlated with the location and intensity of the center of WPSH. The day-to-day variations of ozone mixing ratios are characterized by noticeable HOP that typically lasted for 3–5 days with daily peaking ozone levels exceeding 102 ppb (Chinese air quality standard for ozone) and LOP with daily peaking ozone levels lower than 20 ppb. When the center of WPSH with weaker intensity is to the southeast of Chongming site, the mixing ratios and variability of surface ozone are higher. When the center of WPSH with stronger intensity is to the northeast of Chongming site, the mixing ratios and variability of surface ozone are lower. The vertical profiles of air temperature and RH show that inversion layer occurs at the ground layer during HOP. On one hand, the inversion layer is favorable for accumulation of primary pollutants such as CO in the boundary layer during HOP. On the other hand, the inversion layer weakens the intensity of WPSH by preventing subsidence flow and decreases the air density due to its relatively high temperature. As a result, the inversion layer causes reductions in surface pressure, which explains negative correlation between ozone and surface pressure at the site. Local anthropogenic emissions make significant contributions to surface ozone concentrations only when the center of WPSH is to the southeast of Chongming with reduced intensity and weaker subsidence. During LOP, southeasterly wind carries relatively clean marine air mass to Chongming unfavorable for local photochemical production of ozone, while southwesterly wind during HOP carries aged urban pollution plumes from YRD to Chongming resulting in the incidence of high levels of O_3. Sensitivity simulations using the GEOS-Chem chemical transport model confirm that meteorological condition associated with WPSH is the primary contributor to ozone pollution events observed at Chongming in August.

The EASM has a considerable influence on the weather over East China. In August, the WPSH, which is one of the most important components of EASM, is the crucial weather system affecting the weather over YRD region resulting in enhancement of surface ozone mixing ratios. The analysis of our work suggests that strategies to minimize ozone pollution over YRD region and Shanghai in summer should focus on the times when the intensity of WPSH are observed or predicted to

weaken due to the occurrence of the inversion or isothermal layer in the surface layer and when winds turn westerly. Reduction in emissions of O_3 precursors during such times is likely to be most cost effective measures to reduce summertime incidence of high levels of O_3 over this region.

Jingwei He, PhD candidate, School of Environment, Tsinghua University. Research interest: air pollution control. Yuxuan Wang, Associate Professor, Center for Earth System Science, Tsinghua University. Research interest: atmospheric chemistry. Jiming Hao, Professor, School of Environment, Tsinghua University. Research interest: air pollution control. Lulu Shen, Master student, Center for Earth System Science, Tsinghua University. Research interest: atmospheric chemistry. Long Wang, PhD student, School of Environment, Tsinghua University. Research interest: air pollution control.

Acknowledgments This research was supported by the National Science Foundation of China (grant no. 41005060) and by the International Science & Technology Cooperation Program of China (2010DFA21300). We acknowledge the contribution of Dr. J.W. Munger for helping with the initial setup of the instruments.

References

Chang CP, Zhang Y, Li T (2000) Interannual and interdecadal variations of the East Asian summer monsoon and tropical Pacific SSTs, Part I: roles of the subtropical ridge. J Clim 13:4310–4325

Chen D, Wang YX, McElroy MB, He K, Yantosca RM, Le Sager P (2009) Regional CO pollution and export in China simulated by the high-resolution nested-grid GEOS-Chem model. Atmos Chem Phys 9:3825–3839

Cheung VTF, Wang T (2001) Observational study of ozone pollution at a rural site in the Yangtze Delta of China. Atmos Environ 35:4947–4958

Chin M, Jacob DJW, Parrish DD, Doddridge BG (1994) Relationship of ozone and carbon monoxide over North America. J Geophys Res 99:14565–14573

NCC/CMA (National Climate Center, China Meteorological Administration) (2010) Monitoring data http://cmdp.ncc.cma.gov.cn/Monitoring/monsoon.php?ListElem=pw850

Davis JM, Speckman P (1999) A model for predicting maximum and 8 h average ozone in Houston. Atmos Environ 33:2487–2500

Ding YH, Johnny CLC (2005) The East Asian summer monsoon: an overview. Meteor Atmos Phys 89:117–142

Ding YH, Li CY, Liu YJ (2004) Overview of the South China Sea monsoon experiment. Adv Atmos Sci 21:343–360

Ding AJ, Wang T, Thouret V, Cammas JP, Ndlec P (2008) Tropospheric ozone climatology over Beijing: analysis of aircraft data from the MOZAIC program. Atmos Chem Phys 8:1–13

Elminir HK (2005) Dependence of urban air pollutants on meteorology. Sci Total Environ 350:225–237

Eshel G, Bernstein J (2006) Relationship between lagre-scale atmospheric states, subsidence, static stability and ground-level zone in Illinois, USA. Water Air Soil Poll 171:111–133

Foulger BE, Simmonds PG (1993) Ambient temperature gas purifier suitable for the trace analysis of carbon monoxide and hydrogen and the preparation of low-level carbon monoxide calibration standards in the field. J Chromatogr A 630(1–2):257–263

Gao J, Wang T, Ding A, Liu C (2005) Observations study of ozone and carbon monoxide at the summit of mount Tai (1534 m a.s.l.) in central-eastern China. Atmos Environ 39:4779–4791

Hanna SR (1991) Characteristic of ozone episodes during SCCCAMP 1985. J Appl Meteor 30:534–550

Hao JM, Wang LT (2005) Improving urban air quality in China: Beijing case study. J Air Waste Manag 55:1298–1305

Huang SS, Yu ZH (1962) On the structure of the subtropical high and some associated aspects of the general circulation of atmosphere. Acta Meteor Sin 31:339–359 (in Chinese)

Jacob DJ, Logan JA, Yevich RM, Gardner GM, Spivakovsky CM, Wofsy SC, Munger JW, Sillman S, Prather MJ, Rodgers MO, Westberg H, Zimmerman PR (1993) Simulation of summertime ozone over North America. J Geophys Res 98:14797–14816

Li J, Wang Z, Akimoto H, Gao C, Pochanart P, Wang X (2007) Modeling study of ozone seasonal cycle in lower troposphere over east Asia. J Geophys Res 112:D22S25

Lin SJ, Rood RB (1996) Multidimensional flux-form semi-Lagrangian transport schemes. Mon Weather Rev 124(9):2046–2070

Lin W, Xu X, Zhang X, Tang J (2008) Contributions of pollutants from North China Plain to surface ozone at the Shangdianzi GAW Station. Atmos Chem Phys 8:5889–5898

Liu YM, Wu GX (2000) Reviews on the study of the subtropical anticyclone and new insight on some fundamental problems. Acta Meteor Sin 58:500–512 (in Chinese)

Luo C, St John JC, Zhou X, Lam KS, Wang T, Chameides WL (2000) A nonurban ozone air pollution episode over eastern China: observation and model simulations. J Geophys Res 105(D2):1889–1908

Mao H, Talbot R (2004) O3 and CO in New England: temporal variations and relationships. J Geophys Res 109(D2):1304

Mauzerall DL, Narita D, Akimoto H, Horowitz L, Walters S, Hauglustaine DA, Brasseur G (2000) Seasonal characteristics of tropospheric ozone production and mixing ratios over East Asia: a global three-dimensional chemical transport model analysis. J Geophys Res 105:17895–17910

NBS (National Bureau of Statistics of China) (2007) China statistical yearbook 2006. China Statistics Press, Beijing

NCR (National Research Council) (1991) Rethinking the ozone problem in urban and regional air pollution. National Academy Press, Washington

Parrish DD, Trainer M, Holloway JS, Yee JE, Warshawsky MS, Fehsenfeld FC, Forbes GL, Moody JL (1998) Relationships between ozone and carbon monoxide at surface sites in the North Atlantic region. J Geophys Res 103(D11):13357–13376

Pochanart P, Akimoto H, Kajii Y, Potemkin VM, Khodzher TV (2003) Regional background ozone and carbon monoxide variations in remote Siberia/east Asia. J Geophys Res 108(D1):4028

Steiner AL, Davis AJ, Sillman S, Owen RC, Michalak AM, Fiore AM (2010) Observed suppression of ozone formation at extremely high temperature due to chemical and biophysical feedbacks. P Natl Acad Sci USA 107(46):19685–19690

Tao SY, Chen LX (1987) A review of recent research on the East Asian summer monsoon in China. In: Chang CP, Krishnamurti TN (eds) Monsoon meteorology. Oxford University Press, Oxford, pp 60–92

Tao SY, Zhu FK (1964) Variation of the 100 hPa flow pattern in South Asia in summer and the movement of the subtropical anticyclone over the western Pacific. Acta Meteor Sin 34:385–394 (in Chinese)

Wang T, Cheung VTT, Anson M, Li YS (2001) Ozone and related gaseous pollutants in the boundary layer of eastern China: overview of the recent measurements at a rural site. Geophys Res Lett 28:2373–2376

Wang T, Cheung TF, Li YS, Xu XM, Blake DR (2002) Emission characteristics of CO, NO_x, SO_2 and indications of biomass burning observed at a rural site in eastern China. J Geophys Res 107(D12):4157

Wang T, Wong CH, Cheung TF, Blake DR, Arimoto R, Baumann K, Tang J, Ding GA, Yu XM, Li YS, Streets DG, Simpson IJ (2004a) Relationships of trace gases and aerosols and the emission

characteristics at Lin'an, a rural site in eastern China during spring 2001. J Geophys Res 109:D19S05

Wang YX, McElroy MB, Wang T, Palmer PI (2004b) Asian emissions of CO and NO_x: constraints from aircraft and Chinese station data. J Geophys Res 109:D24304

Wang YX, McElroy MB, Jacob DJ, Yantosca RM (2004c) A nested grid formulation for chemical transport over Asia: applications to CO. J Geophys Res 109:D22307l

Wang T, Guo H, Blake DR, Kwok YH, Simpson IJ, Li YS (2005) Measurements of trace gases in the inflow of South China Sea background air and outflow of regional pollution at Tai O, Southern China. J Atmos Chem 52:295–317

Wang T, Ding A, Gao J, Wu WS (2006) Strong ozone production in urban plumes from Beijing. Geophys Res Lett 33:L21806

Wang YX, McElroy MB, Munger JW, Hao JM, Ma H, Nielsen CP, Chen Y (2008) Variations of O_3 and CO in summertime at a rural site near Beijing. Atmos Chem Phys 8:6335–6363

Wang YX, Hao JM, McElroy MB, Munger JW, Ma H, Nielsen CP, Zhang YQ (2010) Year round measurements of O_3 and CO at a rural site near Beijing: variations in their correlations. Tellus B 62B:228–241

Wang Y, Zhang Y, Hao J, Luo M (2011) Seasonal and spatial variability of surface ozone over China: contributions from background and domestic pollution. Atmos Chem Phys 11:3511–3525

Wild O, Prather MJ, Akimoto H, Sundet JK, Isaksen ISA, Grawford JH, Davis DD, Avery MA, Kondo Y, Sachse GW, Sandholm ST (2004) Chemical transport model ozone simulations for spring 2001 over the western Pacific: regional ozone production and its global impacts. J Geophys Res 109:D15S02

Xu J, Zhu Y, Li J (1997) Seasonal cycles of surface ozone and NO_x in Shanghai. J Appl Meteor 36:1424–1429

Xu WY, Zhao CS, Ran L, Deng ZZ, Liu PF, Ma N, Lin WL, Xu XB, Yan P, He X, Yu J, Liang WD, Chen LL (2011) Characteristics of pollutants and their correlation to meteorological conditions at a suburban site in the North China Plain. Atmos Chem Phys 11:4353–4369

Yamaji K, Ohara T, Uno I, Tanimoto H, Kurokawa J, Akimoto H (2006) Analysis of the seasonal variation of ozone in the boundary layer in East Asia using the Community Multi-scale Air Quality model: What controls surface ozone levels over Japan? Atmos Environ 40(10):1856–1868

Zhang Q, Streets DG, Carmichael GR, He KB, Kannari A, Klimont Z, Park IS, Reddy S, Fu JS, Chen D, Duan L, Lei Y, Wang LT, Yao ZL (2009) Asian emissions in 2006 for the NASA UNTEX-B mission. Atmos Chem Phys 14:5131–5153